Available online at www.sciencedirect.com
ScienceDirect
Analytica Chimica Acta 585 (2007) 344–349
ANALYTICA CHIMICA ACTA
www.elsevier.com/locate/aca

Development of a peptide inhibitor-based cantilever sensor assay for cyclic adenosine monophosphate-dependent protein kinase

Hyuk-Sung Kwon [a], Ki-Cheol Han [a], Kyo Seon Hwang [b], Jeong Hoon Lee [b], Tae Song Kim [b], Dae Sung Yoon [b], Eun Gyeong Yang [a,*]

[a] *Life Sciences Division, Korea Institute of Science and Technology, PO Box 131, Cheongryang, Seoul, Republic of Korea*
[b] *Microsystem Research Center, Korea Institute of Science and Technology, PO Box 131, Cheongryang, Seoul, Republic of Korea*

Received 21 October 2006; received in revised form 5 December 2006; accepted 20 December 2006
Available online 4 January 2007

Abstract

A highly sensitive nanomechanical cantilever sensor assay based on an electrical measurement has been developed for detecting activated cyclic adenosine monophosphate (cyclic AMP)-dependent protein kinase (PKA). Employing a peptide derived from the heat-stable protein kinase inhibitor (PKI), a magnetic bead system was first selected as a vehicle to immobilize the PKI-(5–24) peptide for capturing PKA catalytic subunit and the activity assay was applied for indirectly assessing the binding. Synergistic interactions of adenosine triphosphate (ATP) and the peptide inhibitor with the kinase were then investigated by a solution phase capillary electrophoretic assay, and by surface plasmon resonance technology which involved immobilization of the peptide inhibitor. After systemically evaluated by a homogeneous direct binding assay, the ATP-dependent recognition of the catalytic subunit of PKA by PKI-(5–24) was successfully transferred on to the nanomechanical cantilevers at protein concentrations of 6.6 pM–66 nM, exhibiting much higher sensitivity and wider dynamic range than the conventional activity assay. Thus, direct assessment of activated kinases using the cantilever sensor system functionalized with specific peptide inhibitors holds great promise in analytical applications and clinical medicine.

Keywords: Peptide inhibitor; Heat-stable protein kinase inhibitor; Cyclic adenosine monophosphate-dependent protein kinase; Nanomechanical cantilever; Surface plasmon resonance; Capillary electrophoresis; Fluorescence polarization

1. Introduction

Protein kinases direct the activity, localization and overall function of many proteins, and coordinate central cellular processes [1]. Protein kinases are highly dynamic proteins that can toggle between different conformational states, thereby serving as molecular switches [2]. These regulations are tightly controlled, and their malfunctions often result in development of diseases [3]. Cyclic adenosine monophosphate (cyclic AMP)-dependent protein kinase (PKA) regarded as a prototype for protein kinases [4] exists predominantly as an inactive holoenzyme composed of two regulatory and two catalytic subunits in the absence of cyclic AMP. Binding of cyclic AMP dissociates this inactive holoenzyme to release two active catalytic subunits and a dimeric regulatory subunit saturated with cyclic AMP. The catalytic subunit of PKA can also be potently inhibited by the physiological heat-stable protein kinase inhibitor (PKI) protein, which may provide a second level of regulation [5]. The understanding of these complicated kinase regulations requires the identification of activated kinase, which is also useful for diagnostic applications.

Measurements of activated kinase generally rely on signal amplification by phosphorylation of substrates. Kinase activity assays are performed by standard radioactivity-based methods, immunological methods employing phospho-specific antibodies, and fluorescence-based homogeneous methods [6–9]. Although activation of protein kinases is routinely evaluated by these activity assays, direct observation of the activated kinase could provide more information on the state of the enzyme and the kinase-mediated phenomena. Since a fragment of PKI protein, PKI-(5–24) containing 5–24 amino acid residues has been shown to bind the enzyme with strong affinity [10,11], we have attempted to develop sensor assays using this peptide inhibitor by directly capturing the active form of PKA.

* Corresponding author. Tel.: +82 2 958 5178; fax: +82 2 958 5090.
E-mail address: eunyang@kist.re.kr (E.G. Yang).

0003-2670/$ – see front matter © 2007 Elsevier B.V. All rights reserved.
doi:10.1016/j.aca.2006.12.037

Analytical technology advances have aided development of numerous methodologies for monitoring interactions between peptides and proteins. The use of fluorescence polarization (FP)-based solution phase measurements [12–14] and capillary electrophoresis (CE) [15–17] has been well-established in studies of the peptide–protein binding. Despite the operation complexity, surface plasmon resonance (SPR) technology has also been recognized as a powerful tool for biomolecular interaction analyses [18]. Recently, cantilever-based sensors have been emerged as excellent platforms for detecting extremely small forces, mechanical stresses, and mass additions, thus offering promise of sensing biomolecular interactions with unprecedented sensitivity and dynamic range [19,20]. While the earlier reports have demonstrated for detection of airborne components, more recent interest has shifted to detection of solution components by incorporating biomolecular recognition element [21–23]. For detection of specific molecules, the differences of surface stress between the two opposite cantilever surfaces are measured in the static mode, which presents limitations such as a narrow dynamic range and a parasitic deflection. On the other hand, the dynamic mode is used to detect the resonance frequency shift caused by cantilever mechanical properties such as mass and stiffness, considered more advantageous due to its insensitive nature to the drift of signal arising from the parasitic deflection [24,25].

Here, we examined the conditions for setting up a peptide inhibitor-based sensor for the PKA catalytic subunit. We optimized ATP-dependent interactions between PKA and its inhibitor peptide PKI-(5–24), employing magnetic beads, CE, SPR and FP. Then, we fabricated the nanomechanical $Pb(Zr_{0.52}Ti_{0.48})O_3$ (PZT) cantilever previously demonstrated for electrical measurements of the antibody–antigen interaction [25], and successfully utilized for monitoring ATP-dependent PKA binding to PKI-(5–24) immobilized on the sensor by resonant frequency changes.

2. Experimental

2.1. Reagents

PKA catalytic subunit was purchased from Calbiochem (Darmstadt, Germany), poly-L-arginine (poly-Arg) hydrochloride from Sigma–Aldrich (St. Louis, MO, USA), and M-280 streptavidin-coated magnetic beads from Dynal Biotech ASA (Oslo, Norway). Peptides were synthesized by Peptron (Daejeon, Korea). A PKA substrate, LRRASLG (kemptide), was labeled with fluorescein at the N-terminus and denoted as F-kemptide, and a PKA inhibitor peptide, TTYADFIASGRTGRRNAIHD, was modified with N-terminal biotinylation or fluorescein conjugation and denoted as biotin–PKI-(5–24) or F–PKI-(5–24).

2.2. Fluorescence polarization measurements

FP was measured on an LS-50B fluorimeter (Perkin Elmer), with excitation at 488 nm and emission at 520 nm.

2.3. PKA activity assays

Enzymatic phosphorylation reactions were performed in reaction buffer (50 mM Hepes, pH 7.5, 5 mM $MgCl_2$, 1 mM dithiothreitol (DTT)) containing 100 μM ATP with 1 μM of F-kemptide. Reaction mixtures were incubated with PKA at room temperature for 1–20 min. After boiled to terminate the reactions, the samples were diluted to 100 nM of F-kemptide in 50 mM Hepes, pH 7.5, and their FP signals were measured in the absence or presence of poly-Arg. For radioactive assays, 20 μM ATP containing [γ-^{32}P]ATP and 5 μM F-kemptide were included in reactions. After incubation at room temperature for 20 min, the reactions were stopped by addition of trichloroacetic acid and processed by spotting on P81 phosphocellulose paper, followed by washing in water and quantitation using a BAS ^{32}P-image analyzer.

2.4. Magnetic bead-based binding assays

M-280 streptavidin-coated magnetic beads (1 mg) were reacted with 10 μM of biotin–PKI-(5–24) in phosphate buffered saline (PBS) at room temperature for 30 min, followed by washing with PBS. The biotin–PKI-(5–24) bound beads were then immersed in reaction buffer containing PKA with or without 400 μM ATP at room temperature for 1 min, followed by the PKA activity assays of the supernatants at room temperature for 15 min.

2.5. Capillary electrophorsis analyses

CE analyses were carried out on a Beckman P/ACE 5000 CE–LIF system (Beckman-Coulter, Fullerton, CA, USA) as described previously [26]. Fused-silica capillaries of a total length of 27 cm (20 cm from the inlet to the detection window) and 75 μm ID by 375 μm OD (Beckman-Coulter) were used by pretreating with 1N NaOH and rinsing with deionized water and running buffer (50 mM Hepes, pH 7.5, 1 M non-detergent sulphobetaines (NDSB)-195, 0.1% Triton X-100, 10 mM DTT) for 1 min each. After 50 nM F–PKI-(5–24) with or without 110 nM PKA were mixed with varying concentrations of ATP in binding buffer (50 mM Hepes, pH 7.5, 1 M NDSB-195, 0.1% Triton X-100, 10 mM DTT, 5 mM $MgCl_2$), the samples were injected onto the capillary by pressure of 0.5 psi for 1 s, and separations were carried out by applying +10.8 kV at $20 \pm 0.1\,^{\circ}C$.

2.6. Surface plasmon resonance measurements

Binding experiments were performed using a BIAcore 3000 instrument (Biacore, Applied Biosystems). A CM5 sensor chip (Biacore, Applied Biosystems) was first activated by *N*-ethyl-*N*′-(3-dimethylaminopropyl)carbodiimide and *N*-hydroxysuccinimide, and 50 μg ml^{-1} streptavidin dissolved in PBS was coupled to the activated surface. Biotin–PKI-(5–24) dissolved in PBS was then injected onto the streptavidin-coupled channels for 100 s at a flow rate of 5 μL min^{-1}. For binding experiments, PKA in reaction buffer containing ATP was

injected onto the channels for 100 s at a flow rate of 30 μL min^{-1}, followed by washing with reaction buffer for 200 s.

2.7. Fabrication of PZT thin film cantilevers

Nanomechanical PZT cantilevers contain 12 cantilever arrays with dimensions of 50 μm × 150 μm, fabricated as described previously [25]. Briefly, the substrates were prepared by depositing 1.2 μm-thick low-stress silicon nitride (SiN_x) on 100 mm-diameter p-doped Si (1 0 0) wafers with low-pressure chemical vapor deposition. The bottom electrode of Pt/Ta thin film was prepared on the SiN_x/Si substrates by radiofrequency magnetron sputtering, followed by deposition of the 0.5 μm PZT thin film on the substrate by a diol-based sol–gel route. For the metal–ferroelectric–metal capacitor structure, direct current sputtering was used to deposit a Pt layer for the top electrode. After ion milling to etch the Pt for the top electrode, inductively coupled plasma was utilized to etch the PZT for the piezoelectric material. The Pt bottom electrode was also patterned by ion milling, and the bottom SiN_x window was patterned by reactive ion etching, followed by wet etching of the bulk silicon with a KOH silicon etchant. Finally, the cantilever was formed by SiN_x etching with reactive ion etching, and a SiO_2 thin film was deposited for the electrical and chemical passivation layer.

2.8. Cantilever functionalization and PKA binding assays

A 10/50 nm-thick Cr/Au layer was deposited on the bottom SiN_x side of the PZT cantilever using an e-beam evaporator. The cantilever was then cleaned in H_2O_2:H_2SO_4 (1:4, vol/vol) and deionized water. Streptavidin was immobilized on the cleaned surface using calixcrown self-assembled monolayers (SAMs) which can recognize ammonium ions in protein immobilization [27]. After treated with 10 μg/ml streptavidin in PBS at room temperature for 1 h, the cantilever was washed with PBST (PBS with 0.5% Tween 20, pH 7.5) and dried under nitrogen gas. Subsequently, the cantilevers were immersed in PBS containing 5% BSA for 1 h at room temperature, to minimize non-specific binding. The cantilevers were then rinsed with PBST, and treated with 200 nM biotin–PKI-(5–24) in PBS at room temperature for 1 h, followed by washing with PBST and drying under nitrogen gas. The cantilevers immobilized with biotin–PKI-(5–24) were treated with PKA in reaction buffer at room temperature for 30 min. After the cantilevers were rinsed with reaction buffer, the resonant frequency of the cantilevers was measured by a precision impedance analyzer (4294A, Agilent technologies, USA). At off resonance, the cantilever was a capacitor exhibiting a phase angle around −90°. At resonance, the flexural motion gave rise to a peak in the real part of the impedance, and hence a peak in the phase angle due to the directric piezoelectric effect. All the resonant frequencies used in our experiments showed variations of <2%.

3. Results and discussion

3.1. Inhibition assay using FP-based PKA activity measurements

Selective interactions of fluorescently labeled phosphorylated peptides with cationic polyamino acids have been utilized to detect kinase activities by FP measurements [7]. For the PKA activity assay, the F-kemptide substrate was designed to have the net charge of zero including the charge contributed by a fluorescein tag and to become negatively charged upon enzymatic phosphorylation. Upon reaction with PKA, the FP signals of the reaction sample diluted to 0.1 μM F-kemptide increased significantly with increasing concentrations of poly-Arg (Fig. 1A), whereas those of the untreated sample did far less. From these data, 5 μM poly-Arg was chosen for monitoring the time course of the PKA reaction, which showed an increase of FP with time, eventually approaching to a plateau (Fig. 1B). The FP-based activity assay was then utilized for examining the inhibition of PKA by biotin–PKI-(5–24). When F-kemptide was reacted with PKA containing varying concentrations of biotin–PKI-(5–24), the FP readout of the assay decreased with increasing concentrations of the inhibitor (Fig. 2), indicating potent inhibition of PKA activity with an IC50 value of ∼54 nM.

Employing this peptide inhibitor, our initial attempt was directed at setting up a magnetic bead-based PKA capturing system. After biotin–PKI-(5–24) was immobilized on the streptavidin-coated magnetic beads, varying concentrations of the beads were added in reaction buffer containing 13.2 nM

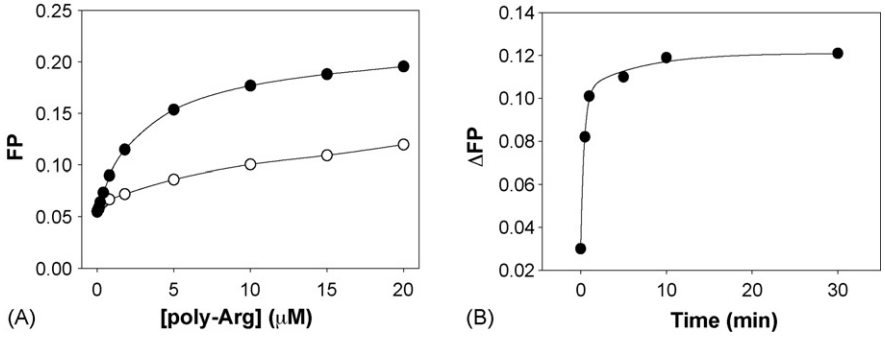

Fig. 1. Detection of PKA activity by FP measurements. (A) F-kemptide at 1 μM was incubated with (●) or without (◯) 13.2 nM of PKA catalytic subunit in reaction buffer containing 100 μM ATP. After the reactions were performed at room temperature for 15 min, FP changes were monitored for the samples diluted to 100 nM of F-kemptide in the presence of increasing concentrations of poly-Arg. (B) FP values were measured in the presence of 5 μM poly-Arg as a function of time of the phosphorylation reaction, and ΔFP values were determined by subtracting FP of the non-reacted F-kemptide from FP of the reacted F-kemptide.

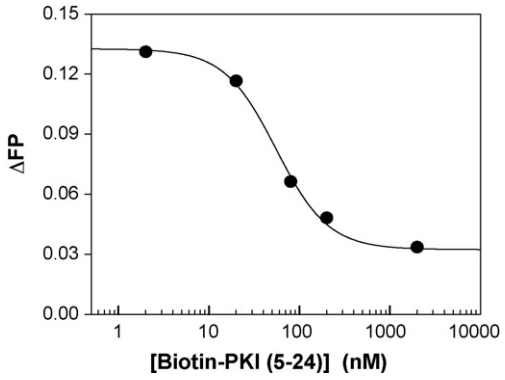

Fig. 2. Inhibition of PKA by biotin–PKI-(5–24). PKA activity assay was performed by incubating 1 μM F-kemptide with 13.2 nM PKA in the presence of the indicated concentrations of the inhibitor peptide at room temperature for 15 min.

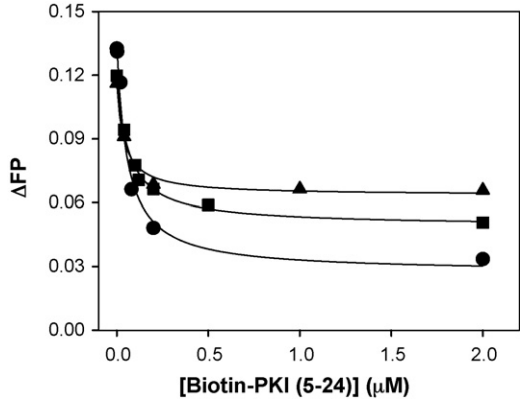

Fig. 3. PKA capturing test using magnetic beads immobilized with biotin–PKI-(5–24). Streptavidin-coated magnetic beads pretreated with biotin–PKI-(5–24) were incubated with PKA in reaction buffer with (■) or without (▲) 400 μM ATP at room temperature for 30 min, and the supernatants were assayed for activity. For a control, inhibitory effects of biotin–PKI-(5–24) on PKA activity were determined in the absence of beads (●).

PKA in the presence or absence of ATP, and the supernatant was assayed for the PKA activity. As shown in Fig. 3, the presence of 400 μM ATP was partially effective in capturing the kinase on the beads, albeit much less than the free PKI-(5–24), indicating that ATP is likely to boost the protein-inhibitor binding. Consistent with these observations, inhibition of PKA by PKI protein has been reported to require the synergistic high-affinity binding of ATP [28]. It should also be noted that the affinity coupling via the biotin–streptavidin interaction was selected as an immobilization protocol, since the epoxy–amine chemical coupling using epoxy magnetic beads did not yield reproducible results (data not shown). However, the magnetic bead-based system was discarded without further optimization due to inefficient capturing of PKA even in the presence of ATP.

3.2. ATP-dependent binding of PKI to PKA examined by CE and SPR

The effects of ATP on the PKI–PKA binding were further examined using F–PKI-(5–24) by CE. To prevent adsorption of the peptide, 1 M NDSB-195 and 0.1% Triton X-100 which had been reported to help reduction of peptide adsorption to the glass wall [29] were included to yield reproducible migration of the peptide. While the mixture of F–PKI-(5–24) and PKA without ATP exhibited a little decrease in the peak, addition of ATP yielded a concentration-dependent decrease of the peptide peak, although the complex peak was not visible (Fig. 4A). On the other hand, no significant change was observed for the F–PKI-(5–24) peptide without PKA in the presence of 500 μM ATP (data not shown). The ATP-dependent binding of PKI with PKA was also evaluated by SPR. After immobilization of biotin–PKI-(5–24) through streptavidin coupled to the CM5 chip surface, 132 nM PKA was injected onto the channels with ATP. As shown in Fig. 4B, the sensorgrams demonstrated ATP-dependent PKI–PKA binding. While the on-rate of PKA increased with increasing concentrations of ATP, PKA dissociated from the peptide inhibitor on the sensor surface more slowly at higher ATP concentrations.

3.3. Direct binding assay based on FP

Employing F–PKI-(5–24), the PKI–PKA binding was further analyzed by FP. With increasing concentrations of ATP, FP increased and leveled off at each fixed kinase concentration (Fig. 5A), and the ATP-dependent binding was most prominent at the highest kinase concentration. In addition,

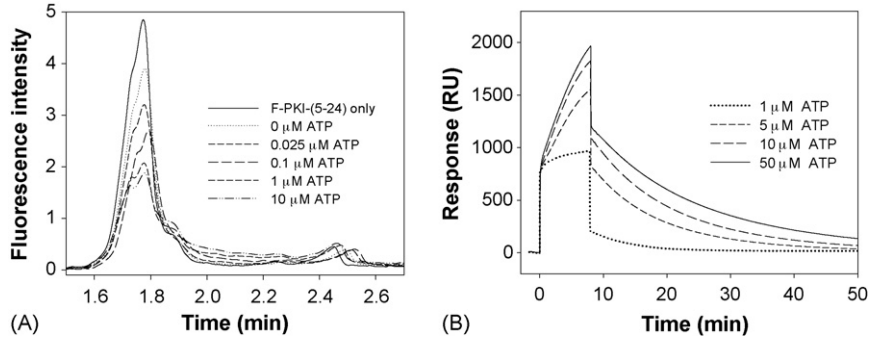

Fig. 4. CE and SPR analyses of the binding between PKA and F–PKI-(5–24). (A) Electropherograms of samples containing 50 nM F–PKI-(5–24) incubated with 110 nM PKA in the presence of increasing concentrations of ATP (0, 0.025, 0.1, 1, and 10 μM) are presented. The highest peak represents F–PKI-(5–24) without PKA. (B) Sensorgrams of PKA binding to the biotin–PKI-(5–24) immobilized chip surface in the presence of increasing concentrations of ATP (1, 5, 10, and 50 μM) are presented.

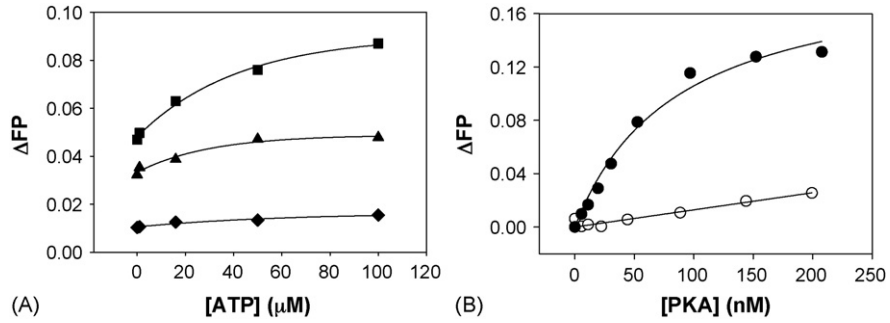

Fig. 5. Interactions between PKA and F–PKI-(5–24) measured by FP changes. (A) The dependence of the complex formation on ATP concentration was analyzed by FP at room temperature for 100 nM F–PKI-(5–24) incubated with 13.2 (♦), 66 (▲) and 132 nM PKA (■). (B) Binding was measured by FP for 50 nM F–PKI-(5–24) incubated with increasing concentrations of PKA in the presence (●) or absence of 100 μM ATP (○).

the binding analysis at a fixed concentration of F–PKI-(5–24) showed that FP increased with increasing concentrations of PKA and approached to a plateau (Fig. 5B), with detection limit of ~10 nM. On the other hand, the interaction between F–PKI-(5–24) and the PKA holoenzyme in the presence of ATP was minimal as observed by the insignificant FP changes (data not shown), which confirms that the PKI peptide could selectively capture the PKA catalytic subunit.

3.4. Cantilever assay

The electrical self-sensing of signal on a cantilever surface presents a convenient method compared to the measurement with an external oscillator. Accordingly, PZT nanomechanical cantilever arrays composed of smart piezoelectric material [25] were fabricated to develop a peptide inhibitor-based biosensor for PKA. Since 12 cantilever arrays of 50 μm × 150 μm were designed in one device, the experimental data from at least six cantilevers were obtained for each sample despite some failures in electrical measurements. After immobilization of streptavidin on the cantilevers functionalized with calixcrown SAMs, followed by binding of biotin–PKI-(5–24) (Fig. 6A), the effect of ATP on the PKI–PKA binding was first tested by treating with 132 nM PKA in reaction buffer in the presence or absence of ATP. The resonant frequency of the treated cantilever repeatedly measured until it reached a saturated value, and subtracted from the frequency of the negative control cantilever yielded a more negative value for the sensors treated with PKA in the presence of ATP; the difference between the samples with and without ATP was more than 300 Hz, supporting that the ATP presence helps the protein-inhibitor binding.

In further exploration of the quantitative aspect of this binding, the magnitude of the resonant frequency change in the presence of ATP was found to increase with increasing concentrations of PKA, whereas the increase of the resonant frequency shift was minimal in the absence of ATP (Fig. 6B). The relative standard deviations for the resonant frequency changes were in the range of 2.8–13%. The analytical sensitivity for

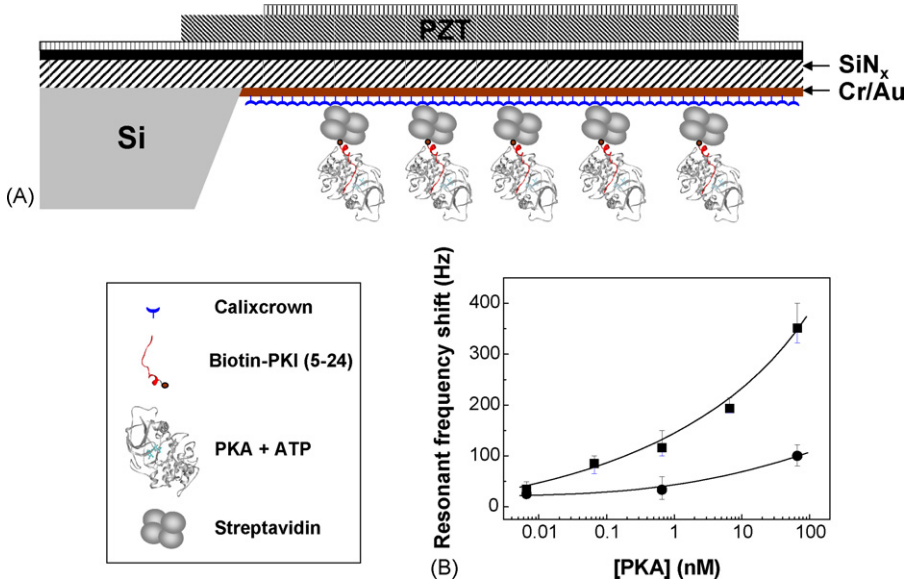

Fig. 6. Nanomechanical detection of PKA catalytic subunit on a funtionalized cantilever. (A) Schematic representation of the binding of on the Au surface of the PZT cantilever funtionalized with biotin–PKI-(5–24) via the biotin–streptavidin interaction. (B) The resonant frequency was measured after incubation with varying concentrations of PKA in the presence (■) or absence of 100 μM ATP (●), and the resonant frequency shift subtracted from the frequency of the negative control cantilever was plotted as a function of the concentration of PKA catalytic subunit. Nanomechanical PZT cantilever devices (5 cm × 5 cm) with 12 arrays of 50 μm × 150 μm were used.

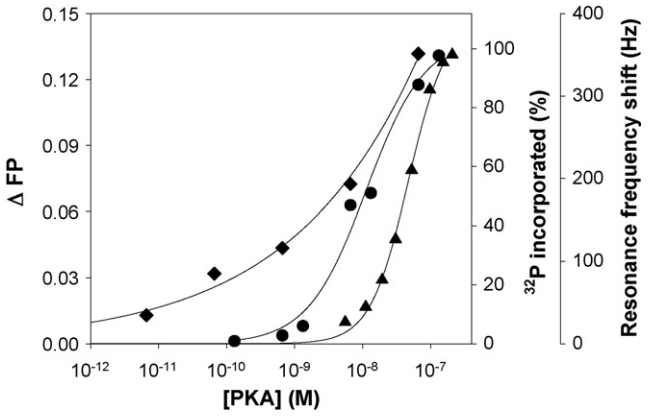

Fig. 7. Comparison of the binding analysis of PKA on the cantilever funtionalized with biotin–PKI-(5–24) (♦) from Fig. 6B, FP-based binding assay (▲) from Fig. 5B, and radioisotope-based activity assay (●).

detecting PKA in the presence of ATP was 6.6 pM, and the resonant frequency appeared to shift more dramatically than expected from theoretical calculations, consistent with the previous data [25]. This was likely originated from the compressive stress exerted by repulsive electrostatic intermolecular interactions or changes in the hydrophobicity on the functionalized side of the cantilever [22]. These results were then compared with a conventional radioactive activity assay using ^{32}P-ATP along with the FP-based binding assay (Fig. 7). In terms of sensitivity, the experimental resonant frequency change resulted from both mass and spring constant variations was superior to the enzymatic amplification of phosphorylation signals or the homogeneous binding detected by FP; the detection limit of the cantilever assay was lower than the radioactive assay and FP-based binding assay by ∼2 and ∼3 orders of magnitude, respectively. In addition, the cantilever assay showed a much larger dynamic range than the other two assay methods. These results suggest that the combination of a cantilever and a specific peptide inhibitor would provide a highly sensitive, label-free sensing system for the active form of PKA. In addition, this peptide inhibitor-based cantilever sensor might be of utility in diagnostics, considering that the active form of PKA has been found to be released from certain carcinoma cell lines [30].

4. Conclusions

Cantilever sensors combined with selective biochemical interactions present revolutionizing potentials for the development of various biosensors. We have employed a peptide inhibitor-baited strategy to capture the active form of PKA, and firmly demonstrated the requirement of ATP for the binding of PKA with PKI-(5–24) by various methods. Feasibility of utilizing the electrical measurements of the resonant frequency change generated on nanomechanical cantilever sensors was then tested for label-free binding assays, which demonstrated that the PKI-(5–24) functionalized cantilever could sense active PKA, when provided with ATP. In addition, quantitative analysis on the cantilevers has proven improved dynamic response and sensitivity over the conventional activity assay, which would allow their use in the future to investigate activated PKA in real samples without amplification or labeling of the samples, thereby reducing the artifacts introduced by these procedures. The concept developed here can significantly expand the scope of applications of the nanomechanical cantilever sensor and provide a novel approach to design simple multi-analyte sensing arrays, for the simultaneous detection of numerous kinases in biological applications.

Acknowledgements

This work was supported by the 21C Frontier Functional Proteomics Research Center funded by the Korean Ministry of Science & Technology, and by the Intelligent Microsystem Center of the 21st Century Frontier R&D Program sponsored by the Korean Ministry of Commerce, Industry and Energy.

References

[1] T. Hunter, Cell 100 (2000) 113.
[2] D.A. Johnson, P. Akamine, E. Radzio-Andzelm, M. Madhusudan, S.S. Taylor, Chem. Rev. 101 (2001) 2243.
[3] P. Cohen, Curr. Opin. Chem. Biol. 3 (1999) 459.
[4] S.S. Taylor, D.R. Knighton, J. Zheng, L.F. Ten Eyck, J.M. Sowadski, Annu. Rev. Cell Biol. 8 (1992) 429.
[5] D.M. Gamm, M.D. Uhler, J. Biol. Chem. 270 (1995) 7227.
[6] R. Seethala, R. Menzel, Anal. Biochem. 255 (1998) 257.
[7] J. Coffin, M. Latev, X. Bi, T.T. Nikiforov, Anal. Biochem. 278 (2000) 206.
[8] J.E. Scott, J.W. Carpenter, Anal. Biochem. 316 (2003) 82.
[9] J.R. Beasley, P.M. McCoy, T.L. Walker, D.A. Dunn, Assay Drug Dev. Technol. 2 (2004) 141.
[10] F.W. Herberg, S.S. Taylor, Biochemistry 32 (1993) 14015.
[11] W. Wen, S.S. Taylor, J. Biol. Chem. 269 (1994) 8423.
[12] S.S. Pin, I. Kariv, N.R. Graciani, K.R. Oldenburg, Anal. Biochem. 275 (1999) 156.
[13] J.R. Lundblad, M. Laurance, R.H. Goodman, Mol. Endocrinol. 10 (1996) 607.
[14] S.H. Park, R.T. Raines, Methods Mol. Biol. 261 (2004) 161.
[15] B.L. Karger, Curr. Opin. Biotechnol. 3 (1992) 59.
[16] Q.H. Wan, X.C. Le, Anal. Chem. 71 (1999) 4183.
[17] J.W. Cooper, Y. Wang, C.S. Lee, Electrophoresis 25 (2004) 3913.
[18] P. Pattnaik, Appl. Biochem. Biotechnol. 126 (2005) 79.
[19] T. Thundat, R.J. Warmack, G.Y. Chen, D.P. Allison, Appl. Phys. Lett. 64 (1994) 2894.
[20] T. Thundat, E.A. Wachter, S.L. Sharp, R.J. Warmack, Appl. Phys. Lett. 66 (1995) 1695.
[21] K.M. Hansen, T. Thundat, Methods 37 (2005) 57.
[22] J. Fritz, M.K. Baller, H.P. Lang, H. Rothuizen, P. Vettiger, E. Meyer, H. Guntherodt, C. Gerber, J.K. Gimzewski, Science 288 (2000) 316.
[23] G. Wu, H. Ji, K. Hansen, T. Thundat, R. Datar, R. Cote, M.F. Hagan, A.K. Chakraborty, A. Majumdar, Proc. Natl. Acad. Sci. USA 98 (2001) 1560.
[24] J.W. Yi, W.Y. Mutharasan, W.-H.J. Shih, J. Appl. Phys. 93 (2003) 619.
[25] J.H. Lee, K.S. Hwang, J. Park, K.H. Yoon, D.S. Yoon, T.S. Kim, Biosens. Bioelectron. 20 (2005) 2157–2162.
[26] K.-C. Han, J. Yu, E.G. Yang, Electrophoresis 26 (2005) 4379.
[27] Y. Lee, E.K. Lee, Y.W. Cho, T. Matsui, I.-C. Kang, T.-S. Kim, M.H. Han, Proteomics 3 (2003) 2289.
[28] J. Lew, N. Coruh, I. Tsigelny, S. Garrod, S.S. Taylor, J. Biol. Chem. 272 (1997) 1507.
[29] C.B. Cohen, E. Chin-Dixon, S. Jeong, T.T. Nikiforov, Anal. Biochem. 273 (1999) 89.
[30] Y.S. Cho, Y.G. Park, Y.N. Lee, M.-K. Kim, S. Bates, L. Tan, Y.S. Cho-Chung, Proc. Natl. Acad. Sci. USA 97 (2000) 835.